Artificial receptor-functionalized nanoshell: facile preparation, fast separation and specific protein recognition

2010 Nanotechnology 21 185502

(http://iopscience.iop.org/0957-4484/21/18/185502)

Nanotechnology **21** (2010) 185502 (9pp) doi:10.1088/0957-4484/21/18/185502

Artificial receptor-functionalized nanoshell: facile preparation, fast separation and specific protein recognition

Ruizhuo Ouyang, Jianping Lei[1] and Huangxian Ju[1]

Key Laboratory of Analytical Chemistry for Life Science (Education Ministry of China), Department of Chemistry, Nanjing University, Nanjing 210093, People's Republic of China

E-mail: jpl@nju.edu.cn and hxju@nju.edu.cn

Received 14 December 2009, in final form 18 March 2010
Published 14 April 2010
Online at stacks.iop.org/Nano/21/185502

Abstract

This work combined molecular imprinting technology with superparamagnetic nanospheres as the core to prepare artificial receptor-functionalized magnetic nanoparticles for separation of homologous proteins. Using dopamine as a functional monomer, novel surface protein-imprinted superparamagnetic polydopamine (PDA) core–shell nanoparticles were successfully prepared in physiological conditions, which could maintain the natural structure of a protein template and achieved the development of molecularly imprinted polymers (MIPs) from one dimension to zero dimension for efficient recognition towards large biomolecules. The resultant nanoparticles could be used for convenient magnetic separation of homologous proteins with high specificity. The nanoparticles possessed good monodispersibility, uniform surface morphology and high saturation magnetization value. The bound amounts of template proteins measured by both indirect and direct methods were in good agreement. The maximum number of imprinted cavities on the surface of the bovine hemoglobin (Hb)-imprinted nanoshell was 2.21×10^{18} g^{-1}, which well matched their maximum binding capacity toward bovine Hb. Both the simple method for preparation of MIPs and the magnetic nanospheres showed good application potential in fast separation, effective concentration and selective biosensing of large protein molecules.

(Some figures in this article are in colour only in the electronic version)

1. Introduction

Currently the preparation of functionalized magnetic nanoparticles, especially high superparamagnetic nanoparticles, with respect to their application in various fields of biomedical diagnostics, concentration and separation of trace amounts of specific targets, and signal amplification, has attracted considerable interest [1–3]. Many natural receptor-functionalized magnetic nanoparticles have been used for the recognition of proteins [4–7] and nucleic acids [8, 9]. However, the use of these expensive receptors such as antibodies, enzymes or nucleic acids limits the extensive applications of functionalized magnetic nanoparticles to a great extent. Thus, it is urgent to explore new artificial recognition elements instead of natural receptors for the functionalization of magnetic nanoparticles.

Molecular imprinting technology has been proven to be an attractive method for the preparation of artificial receptors with predetermined recognition toward target molecules. The resulting receptors have good binding affinity, stability and specificity toward the target molecules, and thus have been widely applied in separation science [10–12], biotechnology [13–15], chemsensing [16–19], analytical chemistry [20, 21], catalysis [22, 23] and drug delivery [24–26]. Although the imprinting of small molecules has been well established and considered almost routine work, only a few molecules such as theophylline, tryptophan 2,4-diclorophenoxyacetic acid, triazine, aspirin and bisphenol A-imprinted polymers have been used for the functionalization of magnetic nanoparticles [27–32]. In the presence of an external magnetic field, the introduction of a magnetic component in the MIPs can allow magnetic separation to replace the centrifugation and

[1] Authors to whom any correspondence should be addressed.

filtration step. However, the imprinting of biomacromolecules such as proteins poses significant challenges due to their large molecular sizes, structural complexity and environmental sensitivity [33–35]. To address these problems, some strategies have been developed for efficient protein imprinting by using surface imprinting technology and new monomers [36–39]. One of the monomers is dopamine (DA), which has been used for the preparation of surface protein-imprinted nanowires with a relatively complicated procedure in our previous work [37]. More recently, a surface protein-imprinted magnetic nanoparticle has also been presented by polymerization of DA in alkaline solution containing hemoglobin (Hb) [38].

This work introduced silanol-modified superparamagnetic nanospheres (PNs) as the core for the preparation of surface protein-imprinted polymers in physiological conditions. This synthesis procedure is much simpler than that of magnetic ribonuclease A surface-imprinted particles [39] due to the adsorption of DA monomer on silanol-modified PNs [40]. More importantly, different from the previous work [38], the imprinting in physiological conditions could maintain the natural structures of the protein templates. By using bovine and human Hb as the models of two homologous proteins, the prepared surface protein-imprinted superparamagnetic polydopamine (PDA) nanospheres not only showed good dispersibility, narrow nanoparticle size and pore distribution, and uniform surface morphology, but also possessed good recognition ability and high binding capacity. This work provided a path to prepare an excellent matrix for fast recognition, separation and concentration of large homologous protein template molecules.

2. Experimental details

2.1. Materials

DA, ammonium persulfate (APS), and human and bovine Hb were purchased from Sigma (St Louis, MO, USA) and used as received. Bovine serum albumin (BSA), ribonuclease A, horseradish peroxidase (HRP) and streptavidin were purchased from Promega (USA) and used as received. Sodium dodecyl sulfate (SDS) was purchased from Jiangsu Huakang Company (Nanjing, China). Silanol-modified core–shell polystyrene microsphere PNs with a mean diameter of 500 nm (diameter range from 420 to 540 nm) were obtained from BaseLine Chromtech Research Centre (Tianjin, China). Phosphate buffer solutions (PBS) with different pHs were prepared by mixing 50 mM aqueous solution of sodium dihydrogen phosphate (NaH_2PO_4) and 50 mM aqueous solution of disodium hydrogen phosphate (Na_2HPO_4). Double-distilled water was used for preparation of all aqueous solutions. BCA-100 protein quantitative analysis kit was purchased from Shenergy Biocolor BioScience and Technology Company (Shanghai, China).

2.2. Preparation of artificial receptor-functionalized PDA nanoshell

DA as a functional monomer was mixed with bovine Hb as the template under stirring at 25 °C to obtain a solution (pH 7.35) containing 0.05 M DA and 1.0 mg ml^{-1} bovine Hb. 0.5 ml of 10 mg ml^{-1} PN aqueous suspension (pH 7.35 PBS) was then added to the solution with a total volume of 20 ml. After adding APS at the molar ratio of 3:1 for DA to APS, the chemical polymerization of DA was initiated. The polymerization process was kept at 25 °C for 4.0 h and at 45 °C for 2.0 h to produce protein-incorporated PDA core–shell PNs, which were then separated from the aqueous solution with a magnet, followed by washing with 10% SDS solution to remove bovine Hb molecules. After that, the bovine Hb-imprinted PDA PNs (IPPNs) were finally obtained. With the same procedure, the human Hb-IPPNs and non-imprinted PDA PNs (NIPPNs) were prepared in the presence and absence of human Hb.

2.3. Analysis of template proteins

The obtained protein-IPPNs were used to recognize the template proteins. Different amounts of the protein-IPPNs or NIPPNs were added to 1.5 ml of 300 μg ml^{-1} protein solution in the presence of 0.01% Tween-20, and oscillated for 2.5 h at 25 °C. After the convenient magnetic separation of protein-IPPNs or NIPPNs from the solution, the concentrations of proteins in the supernatants were determined using a UV-3600 spectrophotometer. The binding amounts of template proteins to protein-IPPNs were calculated by the difference between total template amount and residual amount in solution. At the same time, the binding amounts were also directly determined with a BCA-100 protein quantitative analysis kit using BSA as standard.

2.4. Characterization

The morphology of nanospheres was examined with a Hitachi S-3000N scanning electron microscope (SEM) and x-ray photoelectron spectroscopic (XPS) measurements were performed with an ESCALab MK2 spectrometer. A monochromatic Al Kα x-ray source was operated in CAE (constant analyzer energy) mode (CAE = 100 eV for a survey spectrum and 20 eV for O 1s spectrum). Magnetization measurements were carried out with a Quantum Design MPMS-5S superconducting quantum interference device magnetometer. Nitrogen adsorption–desorption isotherms and pore size distributions were measured using a Micrometeritics ASAP 2020 system. FT-IR spectra were recorded on a NEXUS model 870 Fourier transform IR spectrophotometer (Thermo Electron Corp., MA).

3. Results and discussion

3.1. Preparation and composition of non-imprinted PDA nanoshell

PDA coating is easy to form on the surface of silica via self-polymerization due to the coexistence of catechol and amine groups [40], so the silanol-modified PNs (mean diameter of 500 nm) as magnetic cores were used to produce non- or protein-imprinted PDA nanospheres. First, in the absence of template protein, the monomer DA adsorption on the PNs

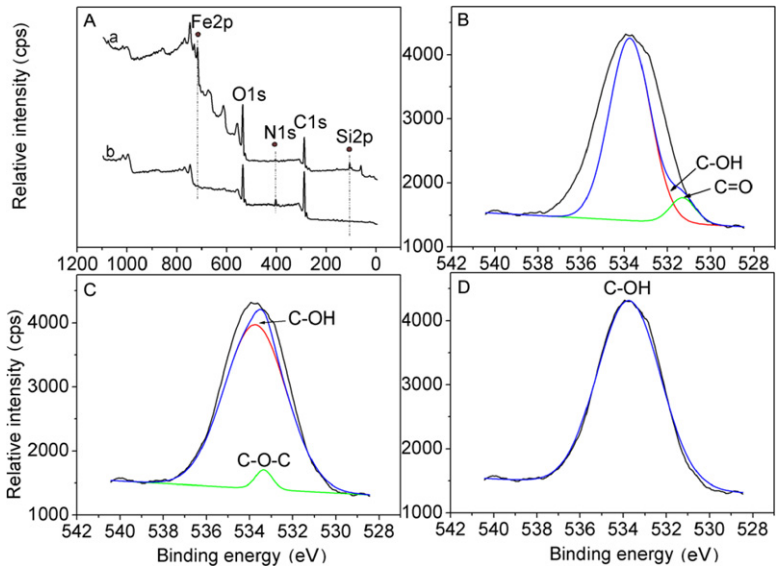

Figure 1. Spectra of (A) survey XPS of (a) silanol-modified PNs and (b) PDA core–shell PNs, and O 1s peak fitted with (B) C=O and C–OH, (C) C–O–C and C–OH, and (D) C–OH.

was initiated by APS to chemically polymerize in neutral pH, thus leading to the formation of PDA nanoshells. XPS characterization was used to monitor the formation of PDA nanoshells (figure 1). The survey spectrum of silanol-modified PNs showed the Si 2p peak at 105.81 eV and the Fe 2p peak at 716.05 eV due to the incompletely coated magnetic core of Fe_3O_4 (figure 1(A), curve (a)). After the polymerization of DA on the surface of silanol-modified PNs, the peaks of both Si 2p and Fe 2p completely disappeared and a new peak of N 1s at 401.06 eV was clearly observed in the survey spectrum (figure 1(A), curve (b)). Moreover, the ratio of nitrogen-to-carbon (N/C) peak areas was 0.11, which was near to the theoretical value of 0.125 of DA, indicating the polymer shell on the surface of silanol-modified PNs was formed from the polymerization of DA [40]. Additionally, the fitted O 1s spectrum could not well match the original O 1s XPS spectrum when either C=O at 531.26 eV (figure 1(B)) or C–O–C at 533.34 eV (figure 1(C)) was combined with a C–OH group at 533.71 eV to fit the spectrum, respectively, whereas when only a C–OH group at 533.71 eV was used to fit the curve, they could well match (figure 1(D)) [41]. These results indicated that the oxygen-containing group in the PDA shell mostly existed as hydroxyl groups.

The existence of hydroxyl groups in the network of the PDA shell was further verified with the FT-IR spectrum (figure 2). The spectrum showed an intensive absorption peak attributed to the stretching vibration of O–H at 3184 cm^{-1} and three moderately intensive peaks assigned to the in-plane and out-of-plane bending vibrations of O–H and stretching vibration of C–OH at 1300, 750 and 1106 cm^{-1}, respectively. In addition, the network showed the stretching vibration of N–H peaked at 3360 cm^{-1} and two typical absorption peaks of phenyl group at 1511 and 1616 cm^{-1} [42]. All these groups provide multifunctional binding sites to template molecules by hydrogen and π–π bonds within the PDA structure,

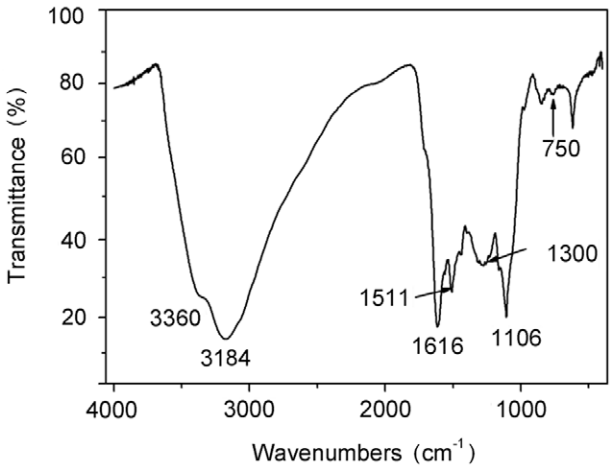

Figure 2. FT-IR spectrum of PDA shell.

which is favorable for obtaining high imprinting and rebinding efficiency.

3.2. Optimization of preparation conditions

The protein-imprinted PDA PNs were then designed and prepared. As shown in scheme 1, the monomer DA adsorption on silanol was initiated by APS to chemically polymerize in neutral pH, during which the template protein molecules were incorporated into the formed network of the PDA shell. In order to obtain efficient protein recognition, the preparation conditions of protein-imprinted PDA core–shell PNs, including the concentrations of DA and template protein, the molar ratio of DA to APS, the polymerization time and the washing time with 10% SDS, were optimized as discussed below in detail using bovine Hb-IPPNs as the model.

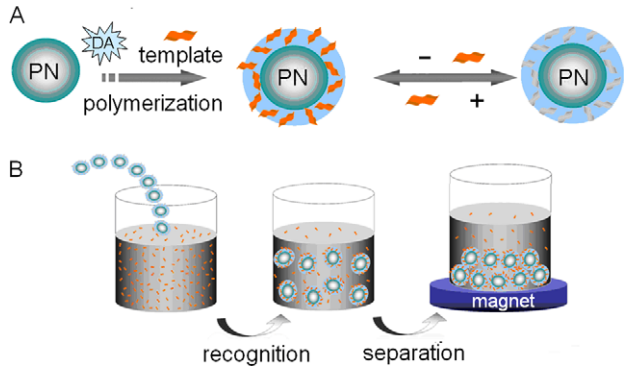

Scheme 1. Illustration of (A) preparation of protein-IPPNs, recognition and (B) separation of protein with the IPPNs.

3.2.1. Concentrations of DA, Hb and APS. DA is an excellent candidate as a functional monomer for protein imprinting due to good biocompatibility and multifunctional groups. As shown in figure 3(A), the binding amount of template protein to the resulting IPPNs obviously increased with the increasing DA concentration used for preparation of the IPPNs, and reached a maximum binding amount at 0.05 M. When the DA concentration was higher than 0.05 M, the increasing thickness of the PDA shell blocked the site accessibility and led to the decrease in the binding amount of bovine Hb. Similarly, the effect of bovine Hb concentration was also examined. As shown in figure 3(B), the best recognition behavior was achieved at the bovine Hb concentration of 1.0 mg ml^{-1}.

The increasing ratio of DA to APS obviously improved the binding ability of the resulting IPPNs to bovine Hb before the ratio of 3:1 (figure 3(C)). Afterwards, the recognition ability gradually decreased due to the gradually incomplete polymerization of DA. Therefore, the chemical polymerization of DA was initiated by APS at the molar ratio of 3:1.

3.2.2. Polymerization time. After the addition of APS, the chemical polymerization of DA was initiated at 25 °C to form a cross-linking structure of PDA [40]. This system was kept at this temperature for a selected time and followed at 45 °C for increasing the cross-linking degree of the polymer. As shown in figures 3(D) and (E), the binding amount of bovine Hb remarkably increased with the increasing polymerization time at 25 °C (figure 3(D)). At 4.0 h, the imprinted cavities

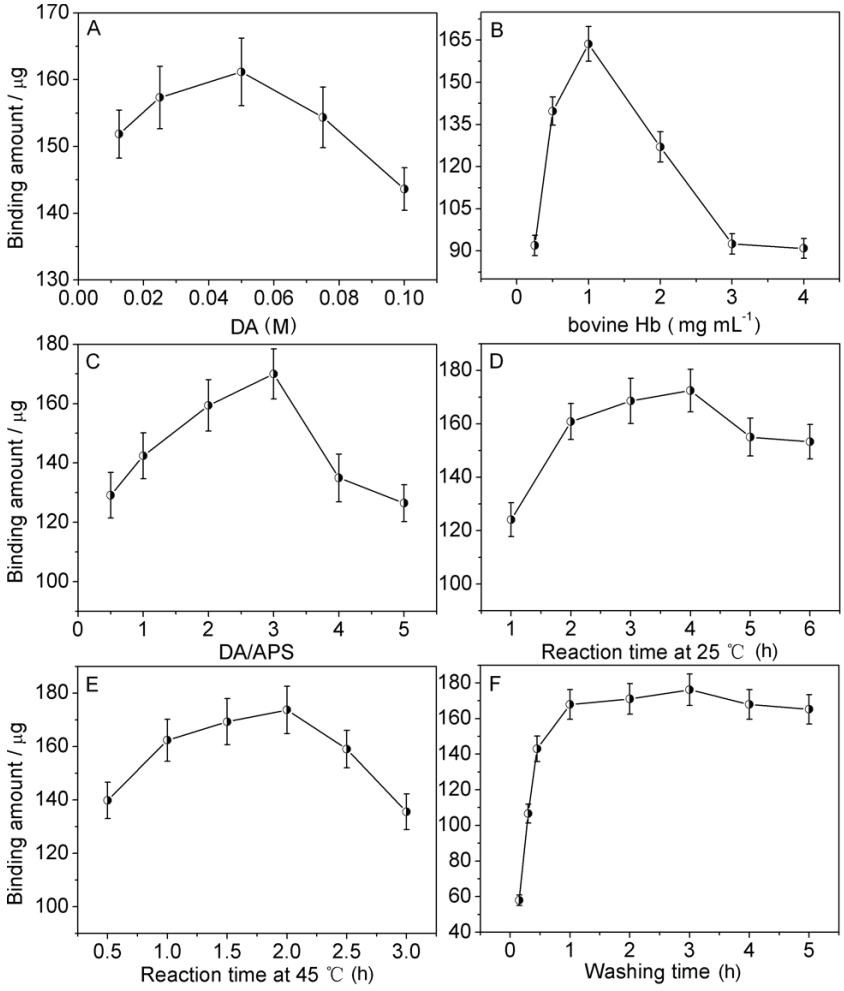

Figure 3. Effects of (A) DA and (B) bovine Hb concentrations, (C) molar ratio of DA to APS, (D) polymerization time of DA at 25 °C and (E) followed at 45 °C, and (F) washing time with 10% SDS on the recognition behavior of bovine Hb-IPPNs towards bovine Hb. IPPN concentration is 2.0 mg ml^{-1} with a volume of 1.5 ml.

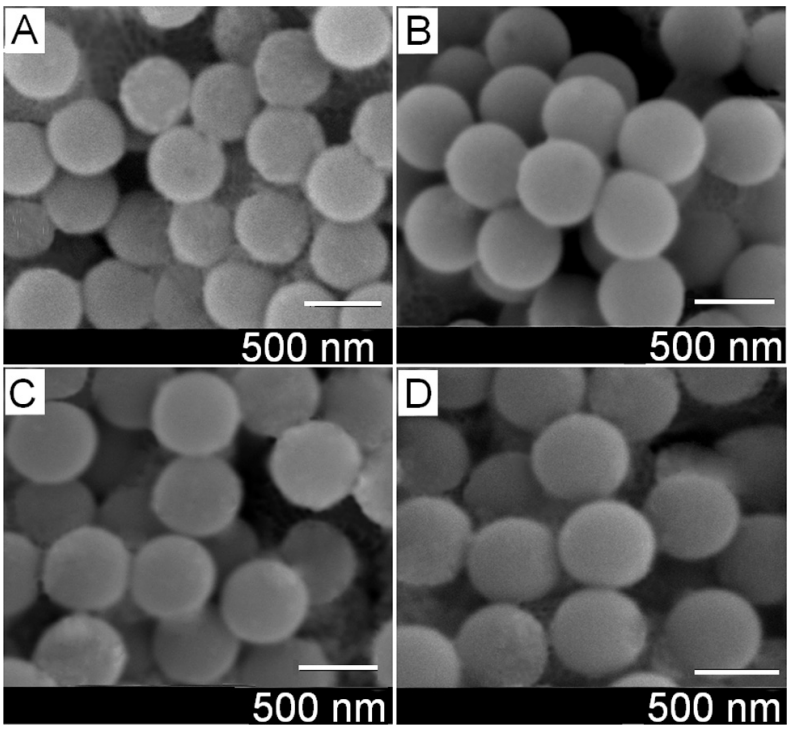

Figure 4. SEM images of (A) silanol-modified PNs, (B) NIPPNs and (C) bovine Hb-IPPNs before and (D) after extracting the template molecules.

showed an optimal recognition performance toward bovine Hb. Longer time would increase the thickness of the PDA shell on the surface of PNs, leading to poor site accessibility of imprinted cavities for template protein. The optimal reaction time at 45 °C for surface imprinting of bovine Hb was 2.0 h (figure 3(E)). When the time was more than 2.0 h, the imprinting efficiency of bovine Hb in the shell was apparently weakened due to the too high degree of cross-linking of the PDA shell, which made the removal of template from the network of the PDA shell more difficult [34].

3.2.3. Washing time of bovine Hb-IPPNs. 10% SDS solution was used to remove the template molecules from the network of the PDA shell (figure 3(F)). With the washing going on, more and more template molecules were extracted from the shell, which was confirmed by the increasing rebinding amount of bovine Hb to IPPNs. At the extracting time of 3 h, the rebinding amount reached the maximum value. When the washing time was continuously prolonged, the imprinted cavities could be partly destroyed.

3.3. Characterization of surface morphology

Figure 4 shows the SEM images of silanol-modified PNs, NIPPNs and as-prepared bovine Hb-IPPNs. The PNs showed acceptable monodispersibility both before and after the formation of the PDA shell or protein-incorporated PDA shell. The PDA core–shell PNs showed slightly larger diameter and more uniform surface morphology than that of the silanol-modified PNs. Furthermore, the removal of template molecules (figure 4(D)) did not obviously change the surface morphology of IPPNs, as compared with that of protein-incorporated PDA core–shell PNs (figure 4(C)). These results showed that the different recognition behaviors of NIPPNs and IPPNs towards the template proteins resulted from the efficient 'footprints', not their morphologic differences. The good monodispersibility of the IPPNs was helpful for the fast diffusion of template protein molecules to the surface of the imprinted PDA shell.

3.4. Magnetic characterization

A similar centrosymmetric shape was observed from the curves of magnetization versus applied magnetic field for silanol-modified PNs, NIPPNs and bovine Hb-IPPNs (figure 5(A)), which was characteristic of the superparamagnetic property. That is, these materials could respond magnetically to an external magnetic field and the response vanished upon removal of the field. The saturation magnetization (S), the maximum magnetic strength, of silanol-modified PNs was 5.7 emu g^{-1}. After encapsulation with PDA and the imprinted PDA shells, the S values of the resulting core–shell particles dropped to 4.4 and 4.6 emu g^{-1}, respectively, which indicated that the PDA shell effectively acted as a shield on the magnetic sphere, and the presence of PDA shell and proteins would decrease the relative content of magnetic materials to produce lower magnetic response toward the external magnetic field compared to silanol-modified PNs [39]. In contrast, the removal of bovine Hb from the PDA shell would increase the relative content of magnetic materials. The S value

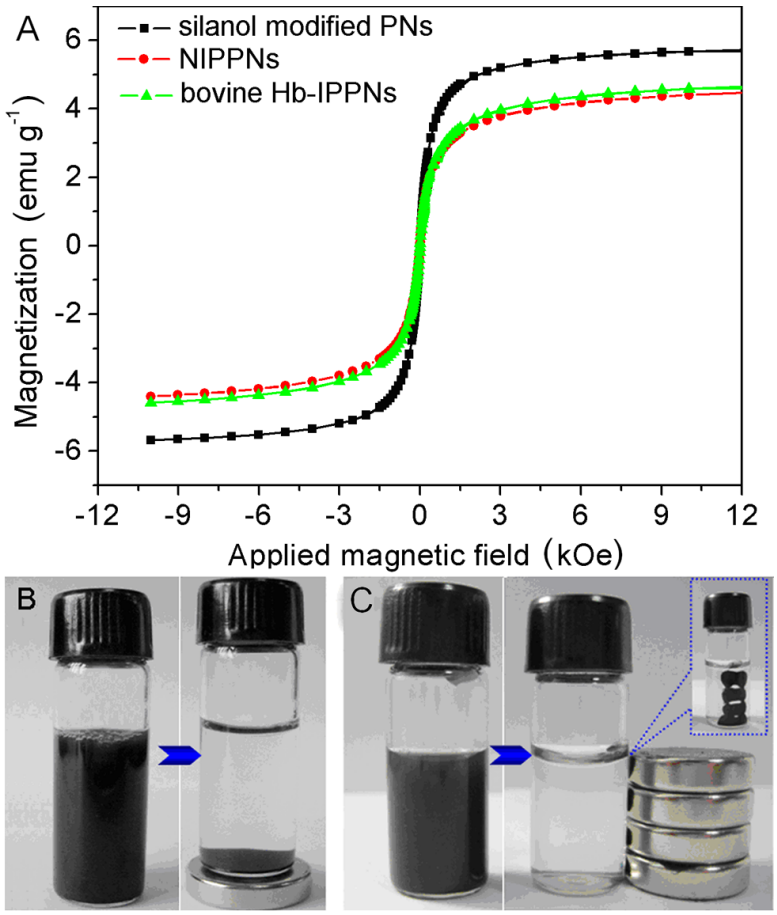

Figure 5. (A) Plots of magnetization versus applied magnetic field for silanol-modified PNs, NIPPNs and bovine Hb-IPPNs, and photos for the magnetic separation of bovine Hb-IPPNs with a magnet placed in (B) the bottom and (C) the side of the bottle.

of the obtained protein-IPPNs was 2.3 times higher than that of 1.97 emu g^{-1} for magnetic theophylline-imprinted nanowires [27], suggesting a sufficient magnetic separation. So after a rebinding process, a complete separation could be observed by putting a magnet in both the bottom (figure 5(B)) and side (figure 5(C)) of the bovine Hb-IPPNs-containing bottle. The inset photo in figure 5(C) confirmed the efficient separation of bovine Hb-IPPNs from the solution.

3.5. Nitrogen adsorption–desorption isotherms

The nitrogen adsorption–desorption isotherms of the silanol-modified PNs, NIPPNs and bovine Hb-IPPNs showed their different pore distributions (figure 6). The amounts of nitrogen adsorbed by NIPPNs and bovine Hb-IPPNs obviously decreased after the silanol-modified PNs was coated with the PDA shell. This indicated that the silanol-modified PNs were mesoporous material and the PDA shell smoothed the surface of PNs, as seen from their SEM images. Although NIPPNs also showed the adsorption of nitrogen, a characteristic of a porous structure, the pore volume was much smaller than that of bovine Hb-IPPNs, indicating the presence of imprinted cavities on the surface of bovine Hb-imprinted PDA shells, which was in good agreement with that of VSM analysis.

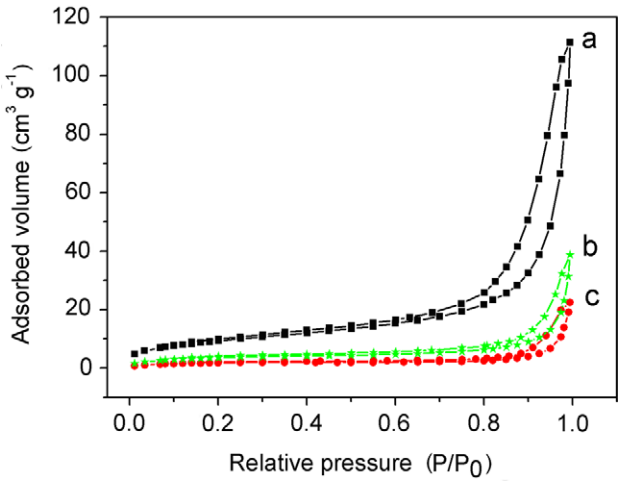

Figure 6. Nitrogen sorption isotherms of (a) silanol-modified PNs, (b) bovine Hb-IPPNs and (c) NIPPNs.

3.6. Effect of pH and ion strength on specific recognition of protein-IPPNs

The effects of pH and ion strength of the binding media were examined for selecting a good binding media for protein recognition (figure 7). The maximum binding amounts of

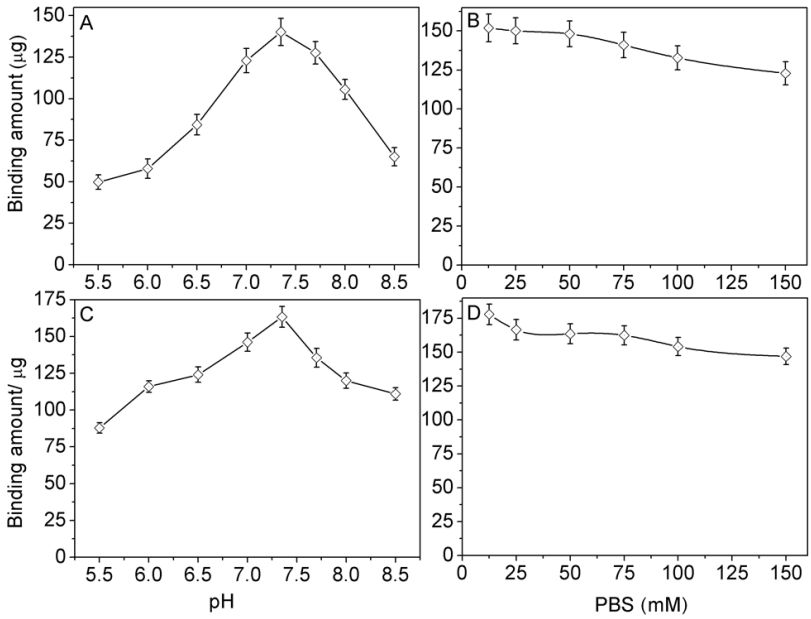

Figure 7. Effects of ((A), (C)) pH and ((B), (D)) ion strength on the recognition behavior of ((A), (B)) bovine and ((C), (D)) human Hb-IPPNs toward individual template proteins. IPPN concentration is 1.0 mg ml^{-1}.

both bovine and human Hb were achieved at pH 7.35 for individual IPPNs (figures 7(A) and (C)). At the same time, no obvious influence of the ion strength was found for two protein-IPPNs in the concentration range of PBS from 12.5 to 150 mM (figures 7(B) and (D)). Hence, 50 mM PBS (pH 7.35) was chosen as the optimal binding media to ensure the binding microenvironment and buffer capacity.

3.7. Binding analysis of bovine and human Hb-IPPNs

Bovine and human Hb-IPPNs were used to investigate the specific recognition performance toward two homologous template proteins under the optimal binding conditions. The binding amounts of template proteins were indirectly calculated from the difference between total and residual amounts of template in the solution, which were measured with a UV spectrophotometer, and directly determined from the rebound Hb-IPPNs with a BCA-100 protein quantitative analysis kit.

Figures 8(A) and (B) show the specific recognition and adsorption curves of bovine and human Hb-IPPNs and NIPPNs toward two individual template proteins, respectively. Both protein-IPPNs displays high binding capacity toward their template proteins (curve (a)) and only small amounts of the two template proteins are bound to NIPPNs due to surface non-specific adsorption (curve (b)), confirming the highly selective recognition ability towards individual template proteins and the good preservation of the native form of the template proteins. Moreover, the binding amounts of two template proteins determined with the direct method are in good agreement with that obtained with the indirect method. Interestingly, good linear binding is observed in the range of low bovine or human Hb-IPPN concentration. With the increasing IPPN concentration the curve trended to a maximum binding amount due to the limited amount of template protein in solution. According to the previously reported equations [37], the selectivity ratios of bovine and human Hb-IPPNs towards corresponding templates are 7.5 ± 1.87 and 8.9 ± 1.44, respectively. The good recognition behaviors could be ascribed to the well-located binding sites within the imprinted cavities and the good monodispersibility of IPPNs as well as the sterically complementary imprinted cavity structure.

The binding amounts of template bovine and human Hb to the IPPNs increased with the increasing protein concentrations with the linear ranges up to 60 and 80 $\mu g\ ml^{-1}$ at the IPPN concentration of 0.3 mg ml^{-1}, respectively (figures 8(C) and (D)). The maximum binding capacities of bovine and human Hb-IPPNs were 266.9 ± 4.4 and 287.0 ± 3.0 mg g^{-1}, i.e. 2.49×10^{18} and 2.68×10^{18} molecules g^{-1}, respectively. Three repeated determinations showed the same maximum binding amounts of the templates. Thus the amounts of templates incorporated and removed from the shell were of the same values.

3.8. Pore size distribution of bovine Hb-IPPNs

The pore size distribution could be calculated from the branches of the nitrogen adsorption–desorption isotherm using the Barrett–Joyner–Halenda method. The pore volumes and mean pore diameters of NIPPNs and bovine Hb-IPPNs were 0.066 ± 0.02 and 0.209 ± 0.22 $cm^3\ g^{-1}$, and 4.60 ± 0.64 and 4.98 ± 1.02 nm, respectively. Comparing with NIPPNs, the relatively high pore volume of bovine Hb-IPPNs could be ascribed to the presence of imprinted cavities. From the mean pore diameter of the imprinted cavities, which was the same as the bovine Hb size of approx. 5.0 nm, and the difference of the pore volumes between bovine Hb-IPPNs and NIPPNs, the total imprinted cavity number of the IPPNs in the PDA shell was calculated to be $2.21 \times 10^{18}\ g^{-1}$. The maximum binding number of bovine Hb in the IPPNs was slightly larger than the

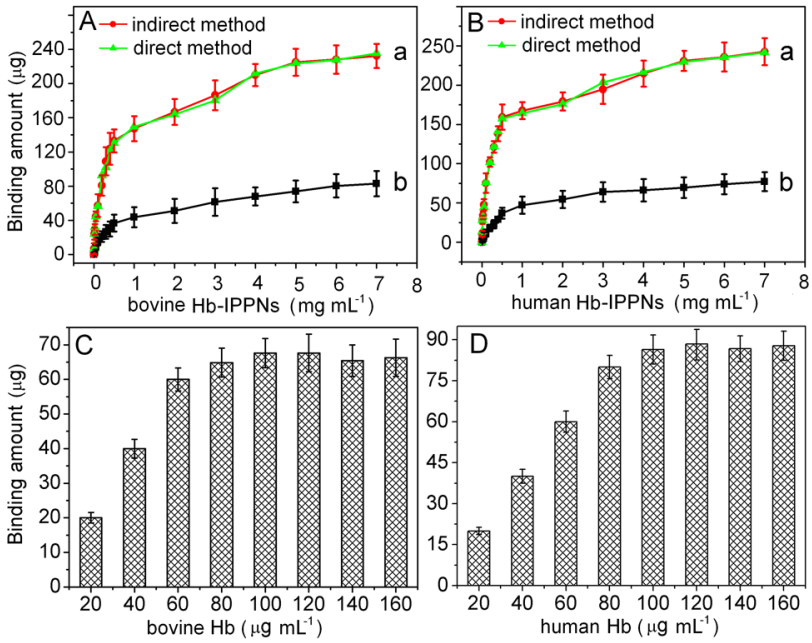

Figure 8. Binding profiles of (A) bovine and (B) human Hb-IPPNs (a) and NIPPNs (b) in 1.5 ml solution containing 450 μg template protein, and the binding amount of IPPNs to (C) bovine and (D) human Hb at different concentrations.

imprinted cavity number due to the non-specific adsorption of Hb molecules on the shell.

3.9. Specificity of bovine and human Hb-IPPNs

Four competing proteins, including BSA, streptavidin, HRP and ribonuclease A, were chosen to examine the specific recognition ability of both bovine and human Hb-IPPNs (figure 9). In the presence of the competing proteins, the relative rebinding of template proteins to IPPNs could still reach above 73%, revealing the high specific selectivity of protein-IPPNs toward the template proteins. The resistance of human Hb-IPPNs against these competitors was slightly stronger than that of bovine Hb-IPPNs, which corresponded to its higher selectivity ratio.

Both Hb-IPPNs showed high specific selectivity toward their template molecules and dramatically low recognition toward other proteins (figure 10). Although the relative binding of bovine Hb to human Hb-IPPNs or human Hb to bovine Hb-IPPNs was slightly higher than those of other heterogeneous proteins due to the analogical structures of homologous proteins, the significant difference between the binding abilities of the IPPNs to template and homologous proteins could be observed, indicating the high specificity and selectivity of the protein-imprinted PDA nanoshells toward template proteins.

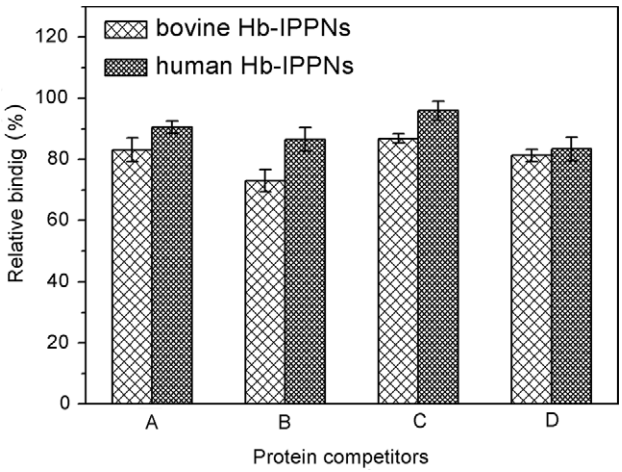

Figure 9. Competitive binding of bovine and human Hb in the presence of competing proteins: (A) BSA, (B) streptavidin, (C) HRP and (D) ribonuclease A to IPPNs at pH 7.35. IPPN concentration is 2.0 mg ml^{-1}.

4. Conclusions

In summary, the surface protein-IPPNs have been prepared via a facile way using silanol-modified PNs as the core in physiological conditions, which have uniform surface, good monodispersibility and high saturation magnetization values for efficient magnetic separation. The diameter and number of the imprinted cavity in the PDA nanoshell are in good agreement with the molecular size and the maximum binding amount of templates to IPPNs. The satisfactory selectivity and specificity of the artificial receptor-functionalized magnetic nanoparticles are due to the polar interactions and steric complementarity of the imprinted cavity, which provides a simple way to quickly distinguish the homologous and heterogeneous proteins and to conveniently separate the large protein templates. These methods could be extended to other biomacromolecules, such as nucleic acid and DNA, for their recognition, separation, concentration and biosensing.

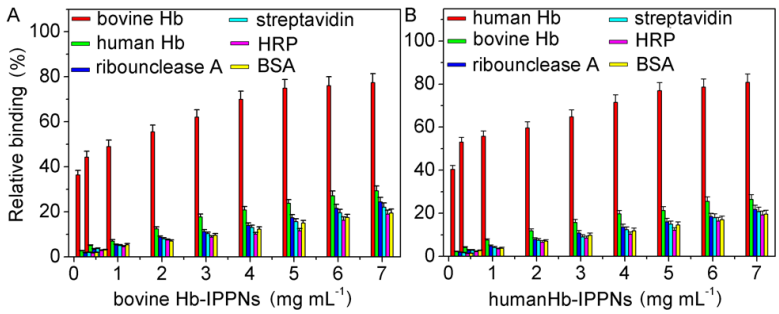

Figure 10. Binding performances of (A) bovine and (B) human Hb-IPPNs toward four competing proteins and two template proteins.

Acknowledgments

This project was supported by the National Science Funds for Creative Research Groups (20821063), the Major Research Plan (90713015), the Key Program (20535010, 20835006) and the General Program (20705012) from the National Natural Science Foundation of China, and the Science Foundation of Jiangsu (BK2008014).

References

[1] Gupta A K and Gupta M 2005 *Biomaterials* **26** 3995
[2] Ceyhan B, Alhorn P, Lang C, Schüle D and Niemeyer C M 2006 *Small* **2** 1251
[3] Grasset F, Molard Y, Cordier S, Dorson F, Mortier M, Perrin C, Guilloux-Viry M, Sasaki T and Haneda H 2008 *Adv. Mater.* **20** 1710
[4] Perez J M, Josephson L, O'Loughlin T, Högemann D and Weissleder R 2002 *Nat. Biotechnol.* **20** 816
[5] Kang H W, Josephson L, Petrovsky A, Weissleder R and Bogdanov A 2002 *Bioconjug. Chem.* **13** 122
[6] Nam J M, Thaxton C S and Mirkin C A 2003 *Science* **301** 1884
[7] Gu H W, Xu K M, Xu C J and Xu B 2006 *Chem. Commun.* 941
[8] Perez J M, O'Loughlin T, Simeone F J, Weissleder R and Josephson L 2002 *J. Am. Chem. Soc.* **124** 2856
[9] Wang J, Liu G D and Merkoci A 2003 *J. Am. Chem. Soc.* **125** 3214
[10] Rao G V, Krug M E, Balamurugan S, Xu H, Xu Q and López G P 2002 *Chem. Mater.* **14** 5075
[11] Smuleac V, Butterfield D A and Bhattacharyya D 2004 *Chem. Mater.* **16** 2762
[12] Mohamed R, Richoz-Payot J, Gremaud E, Mottier P, Yilmaz E, Tabet J C and Guy P A 2007 *Anal. Chem.* **79** 9557
[13] Chu L Y, Yamaguchi T and Nakao S 2002 *Adv. Mater.* **14** 386
[14] Shimoboji T, Larenas E, Fowler T, Kulkarni S, Hoffman A S and Stayton P S 2002 *Proc. Natl Acad. Sci.* **99** 16592
[15] Sharma S, Kaur P, Jain A, Rajeswari M R and Gupta M N 2003 *Biomacromolecules* **4** 330
[16] Li J H, Kenclig C E and Nesterov E E 2007 *J. Am. Chem. Soc.* **129** 15911
[17] Hu X B, Li G T, Huang J, Zhang D and Qiu Y 2007 *Adv. Mater.* **19** 4327
[18] Ayela C, Vandevelde F, Lagrange D, Haupt K and Nicu L 2007 *Angew. Chem. Int. Edn* **46** 9271
[19] Ouyang R Z, Lei J P and Ju H X 2007 *Adv. Funct. Mater.* **17** 3223
[20] Tai D F, Lin C Y, Wu T Z and Chen L K 2005 *Anal. Chem.* **77** 5140
[21] Trammell S A, Zeinali M, Melde B J, Charles P T, Velez F L, Dinderman M A, Kusterbeck A and Markowitz M A 2008 *Anal. Chem.* **80** 4627
[22] Carboni D, Flavin K, Servant A, Gouverneur V and Resmini M 2008 *Chem. Eur. J.* **14** 7059
[23] Liu J Q and Wullf G 2008 *J. Am. Chem. Soc.* **130** 8044
[24] Chilkoti A, Dreher M R, Meyer D E and Raucher D 2002 *Adv. Drug Deliv. Rev.* **54** 613
[25] Zhu Y F, Shi J L, Shen W H, Dong X P, Feng J W, Ruan M L and Li Y S 2005 *Angew. Chem. Int. Edn* **44** 5083
[26] Sellergren B and Allender C J 2005 *Adv. Drug Deliv. Rev.* **57** 1733
[27] Li Y, Yin X F, Chen F R, Yang H H, Zhuang Z X and Wang X R 2006 *Macromolecules* **39** 4497
[28] Lu S, Cheng G, Zhang H and Pang X 2006 *J. Appl. Ploym. Sci.* **99** 3241
[29] Wang X, Ding X, Zheng Z, Hu X, Cheng X and Peng Y 2006 *Macromol. Rapid Commun.* **27** 1180
[30] Zhang Y, Liu R J, Hu Y L and Li G K 2009 *Anal. Chem.* **81** 967
[31] Kan X W, Geng Z R, Zhao Y, Wang Z L and Zhu J J 2009 *Nanotechnology* **20** 165601
[32] Lu C H, Wang Y, Li Y, Yang H H, Chen X and Wang X R 2009 *J. Mater. Chem.* **19** 1077
[33] Haupt K 2003 *Chem. Commun.* 171
[34] Turner N W, Jeans C W, Brain K R, Allender C J, Hlady V and Britt D W 2006 *Biotechnol. Prog.* **22** 1474
[35] Ye L and Mosbach K 2008 *Chem. Mater.* **20** 859
[36] Li Y, Yang H H, You Q H, Zhuang Z X and Wang X R 2006 *Anal. Chem.* **78** 317
[37] Ouyang R Z, Lei J P and Ju H X 2008 *Chem. Commun.* 5761
[38] Zhou W H, Lu C H, Guo X C, Chen F R, Yang H H and Wang X R 2010 *J. Mater. Chem.* **20** 880
[39] Tan C J and Tong Y W 2007 *Anal. Chem.* **79** 299
[40] Lee H, Dellatore S M, Miller W M and Messersmith P B 2007 *Science* **318** 426
[41] Briggs D 1998 *Surface Analysis of Polymers by XPS and Static SIMS* (Cambridge: Cambridge University Press) p 67
[42] Ou J F, Wang J Q, Liu S, Zhou J F and Yang S R 2009 *J. Phys. Chem.* C **113** 20429